

mRNA cap analogues substituted in the tetraphosphate chain with CX₂: identification of O-to-CCl₂ as the first bridging modification that confers resistance to decapping without impairing translation

Anna M. Rydzik^{1,2}, Marcin Warminski¹, Pawel J. Sikorski³, Marek R. Baranowski¹, Sylwia Walczak^{3,4}, Joanna Kowalska¹, Joanna Zuberek¹, Maciej Lukaszewicz¹, Elzbieta Nowak⁵, Timothy D. W. Claridge², Edward Darzynkiewicz^{1,3}, Marcin Nowotny⁵ and Jacek Jemielity^{3,*}

¹Division of Biophysics, Institute of Experimental Physics, Faculty of Physics, University of Warsaw, Zwirki i Wigury 93, 02-089 Warsaw, Poland, ²Chemistry Research Laboratory, University of Oxford, 12 Mansfield Road, Oxford OX1 3TA, UK, ³Centre of New Technologies, University of Warsaw, Banacha 2c, 02-097 Warsaw, Poland, ⁴College of Inter-Faculty Individual Studies in Mathematics and Natural Sciences, University of Warsaw, Zwirki i Wigury 93, 02-089 Warsaw, Poland and ⁵Laboratory of Protein Structure, International Institute of Molecular and Cell Biology, 4 Ksiecia Trojdena Street, 02-109 Warsaw, Poland

Received May 06, 2016; Revised June 14, 2017; Editorial Decision June 17, 2017; Accepted June 20, 2017

ABSTRACT

Analogues of the mRNA 5'-cap are useful tools for studying mRNA translation and degradation, with emerging potential applications in novel therapeutic interventions including gene therapy. We report the synthesis of novel mono- and dinucleotide cap analogues containing dihalogenmethylenbisphosphate moiety (i.e. one of the bridging O atom substituted with CCl₂ or CF₂) and their properties in the context of cellular translational and decapping machineries, compared to phosphate-unmodified and previously reported CH₂-substituted caps. The analogues were bound tightly to eukaryotic translation initiation factor 4E (eIF4E), with CCl₂-substituted analogues having the highest affinity. When incorporated into mRNA, the CCl₂-substituted dinucleotide most efficiently promoted cap-dependent translation. Moreover, the CCl₂-analogues were potent inhibitors of translation in rabbit reticulocyte lysate. The crystal structure of eIF4E in complex with the CCl₂-analogue revealed a significantly different ligand conformation compared to that of the unmodified cap analogue, which likely contributes to the improved binding. Both CCl₂- and CF₂- analogues

showed lower susceptibility to hydrolysis by the decapping scavenger enzyme (DcpS) and, when incorporated into RNA, conferred stability against major cellular decapping enzyme (Dcp2) to transcripts. Furthermore, the use of difluoromethylene cap analogues was exemplified by the development of ¹⁹F NMR assays for DcpS activity and eIF4E binding.

INTRODUCTION

The cap is the characteristic feature present on the 5' end of eukaryotic mRNAs. It consists of 7-methylguanosine connected via 5'-5' triphosphate linkage to the first nucleotide of the mRNA (Figure 1A) (1). The cap structure is involved in mRNA recognition and metabolism including synthesis, transport, translation and turnover (2,3). Therefore, synthetic cap analogues have found a wide range of applications in biological studies, biotechnology and medicine, either as small molecule inhibitors of cap-dependent processes or as reagents for the modification of 5' end of mRNA (4,5). Among variety of cap binding proteins, eIF4E (eukaryotic translation initiation factor) appears to be especially promising candidate for inhibition studies. eIF4E is a constituent of translation initiation complex and its binding to mRNA cap is the first event in protein biosynthesis. Several studies have shown that targeting translation initi-

*To whom correspondence should be addressed. Tel: +48 22 55 43774; Email: jacekj@biogeo.uw.edu.pl

Present address: Anna M. Rydzik, Department of Chemistry, Ludwig-Maximilians University Munich, Butenandtstr. 5-13, 81377 Munich, Germany.

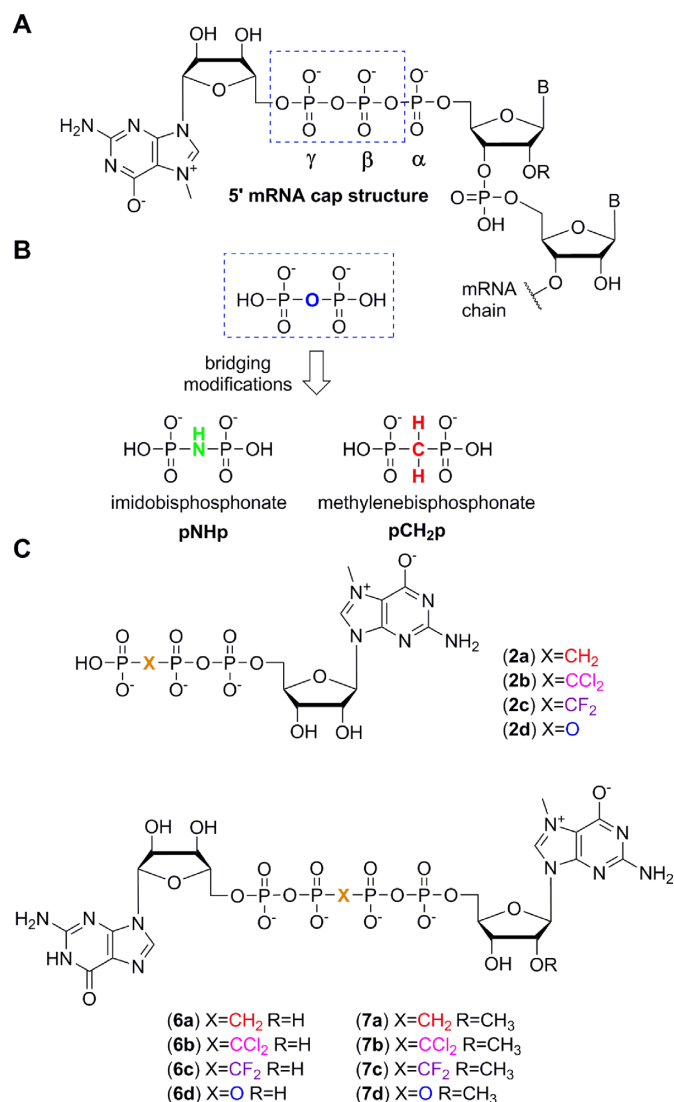


Figure 1. (A) Schematic structure of the mRNA 5'-cap. (B) Imidodiphosphonate (pNHp) and methylenebisphosphonate (pCH₂p) are previously reported substitutions of bridging oxygen in the mRNA 5'-cap. (C) Structures of the mono- and dinucleotide cap analogues used in this study, including newly synthesized pCCl₂p and pCF₂p analogues.

ation machinery is one of possible strategies for development of novel anti-cancer therapies (6–8). Although eIF4E is involved in general cap-dependent translation mechanism in eukaryotic cells, eIF4E overexpression leads to translational upregulation only of a subset of oncogenic transcripts (so called ‘weak’ mRNAs). Consequently, targeting eIF4E by various approaches has been shown to impede tumor growth with minimal or without any toxic effect on healthy cells (9–11).

On the other hand, capped mRNAs have been recently intensively investigated in the context of gene therapy applications and have already entered clinical trials (12–14). For example, it has been shown that dendritic cells can be targeted *in vivo* with intravenously administered RNA-lipoplexes to trigger release of interferon- α (14). Chemically modified cap analogues have been shown to increase

mRNA half-life and translation levels *in vivo*, thereby improving the pharmacological properties of recombinant antigen-encoding RNAs (15). In particular, chemical modifications that stabilize cap analogues against specific decapping pyrophosphatases are of interest (5). Two major decapping enzymes have been identified in the cells: DcpS (decapping scavenger) and decapping complex Dcp1–Dcp2 (16–18). DcpS acts in the 3'-to-5' decay by removing cap structures released after mRNA degradation by the exosome. In contrast, the Dcp1–Dcp2 complex, in which Dcp1 is the regulatory and Dcp2 the catalytic subunit, targets only capped transcripts thereby directing them to the 5'-to-3' decay pathway. However, new enzymes displaying, at least *in vitro*, similar decapping activities are being continuously reported and their biological roles investigated (19–22). The modifications of the triphosphate chain that have been previously employed to prevent decapping include substitutions of non-bridging oxygen atoms with other heteroatoms (S, Se, BH₃) or substitutions of bridging oxygen atoms with methylene (CH₂) or imido (NH) groups (23–26) (Figure 1B). The substitutions in the bridging positions lack the P-stereocenter, which is created in the case of non-bridging substitutions, and thus are easier to produce and purify. Methylenebisphosphonate- (pCH₂p) and imidodiphosphonate (pNHp) isosteres of pyrophosphate are widely used as tools in various binding and enzymatic activity studies (27–33). In general, pNHp is a closer mimic of pyrophosphate, both in respect to the pK_a of phosphate groups and to geometry. However, it suffers from hydrolytic instability, especially in acidic conditions (6,34). On the other hand, the pCH₂p moiety is hydrolytically stable but to larger extent affects the pK_a of neighboring phosphates and cannot be engaged in H-bond interactions (31). This may result in disruption of the polar interactions within protein binding sites (35,36). The previously reported cap analogues containing methylenebisphosphonate (pCH₂p) moiety were characterized by diminished affinity to cap-binding translation initiation factor 4E (eIF4E) (36,37). Consequently, these analogues were relatively poor inhibitors of cap-dependent translation and when incorporated into the 5' end of mRNA, led to poorly translated transcripts. Therefore, in this work investigated another type of pyrophosphate isosteres, dihalogenated bisphosphonates, i.e. difluoro- (pCF₂p) and dichlorobisphosphonate (pCCl₂p). We expected that the electronic effects associated with the electronegativity of fluorine and chlorine, which include lowering the pK_a of phosphonates (30), might improve the protein binding properties of such cap analogues while maintaining their stability toward enzymatic decapping.

Two series of cap analogues were designed: mononucleoside triphosphates (2b–c) and dinucleoside tetraphosphates (6b–c, 7b–c, Figure 1C). In the dinucleotide series, the phosphate linkage was extended from three to four phosphate units in order to increase the binding affinities for eIF4E, as previously demonstrated (35,38). In both series, β/γ -bridging oxygen was chosen as the modification site to yield cap analogues with dichloromethylene and difluoromethylene linkers. The choice of modification site was dictated by synthetic availability and assumption that it could confer stability towards both cap-specific pyrophosphatases DcpS

and Dcp2. In the dinucleotide series the ‘Anti-Reverse Cap Analogs’ (ARCA) (39,40) containing an additional 2'-O-methylation in the 7-methylguanosine moiety (7b-c) were also synthesized. These cap analogues were dedicated for incorporation into mRNA 5' ends by *in vitro* transcription. For comparison, previously reported pCH₂p cap analogues (2a, 6a, 7a) and cap analogues with unmodified phosphate chain (2d, 6d, 7d) were used (Figure 1C).

MATERIALS AND METHODS

Synthesis

Procedures for the synthesis and characterization of the cap analogues are given in the Supporting Information.

pKa measurements

The nucleotides were dissolved in a mixture of H₂O and D₂O (86:14) at concentrations ranging from 3 to 20 mM. The pH of the samples was adjusted in steps of ~0.5 pH units with 100 mM aqueous solution of HCl (containing 16% D₂O) or 100 mM NaOH (16% D₂O). The pH was measured using the HANNA HI1093B pH electrode at 20°C. NMR spectra were obtained on Bruker Avance III 500 MHz spectrometer equipped with a high stability temperature unit using 5 mm PABBO BB/19F-1H/D Z-GRD probe at 471 MHz (¹⁹F NMR) or 202.50 MHz (³¹P NMR). Both ¹⁹F and ³¹P NMR spectra were measured at 25°C. The ³¹P NMR chemical shifts were referenced to 20% phosphorus acid in D₂O (δ_P = 0 ppm) as an external standard. The ¹⁹F NMR chemical shifts were reported to external 10 mM NaF in D₂O (δ_F = -121.5 ppm). The obtained data were processed using OriginLab software and the pK_a values were obtained by fitting to the experimental points a curve described by the following equation:

$$\text{chemical shift} = A_1 + \frac{(A_2 - A_1)}{1 + 10^{(pK_a - pH)*p}}$$

Protein preparation

Mouse eukaryotic initiation factor eIF4E (residues 28–217) and human DcpS (41) were expressed as described before (42). Human Dcp2 was expressed in *Escherichia coli* and purified as described previously (17).

DcpS enzymatic stability assays

A standard sample contained 40 μM cap analogue, 62.5 nM hDcpS in 0.4 ml of 50 mM Tris-HCl pH 7.6 containing 0.2 M KCl, 0.5 mM EDTA, 1.2 mM DTT at 37°C. 100 μl aliquots of the reaction mixture were collected after 15, 30, 60, 120 min and thermally deactivated at 100°C for 3 min. Mixtures containing no hDcpS were used as controls. Control samples were incubated for 120 min at 37°C and then incubated for 3 min at 100°C. All cap analogues in control samples (without DcpS added) were found to be stable after 120 min incubation in the experimental conditions. The samples were stored on ice and analyzed by RP-HPLC using a linear gradient from 0 to 50% of methanol in 0.1 M KH₂PO₄ pH 6.0 within 15 min (UV-detection at 260 nm).

The experiment was performed in duplicate for each analogue.

Percentage hydrolysis was calculated from the following equation:

$$\% \text{hydrolysis} = \frac{q(P_1 + P_2)}{q(P_1 + P_2) + S} \times 100\%$$

where *S* is absorbance of a substrate, *P* the absorbance of a cleavage product and *q* = ε_S/(ε_{P1} + ε_{P2}), where ε_S is extinction coefficient for a substrate, ε_P the extinction coefficient for a product. The extinction coefficients used for calculations were as follows: ε = 22 600 M⁻¹ cm⁻¹ is (dinucleotide analogues containing guanosine and 7-methylguanosine), ε = 11 400 M⁻¹ cm⁻¹ is (mononucleotide analogues containing 7-methylguanosine), ε = 12 080 M⁻¹ cm⁻¹ is (mononucleotide analogues containing non-methylated guanosine). In the case of hydrolysis of dinucleotide analogues *q* = 0.9, for hydrolysis of mononucleotide analogues *q* = 1 and the equation is simplified to % hydrolysis = *P*/(*P* + *S*) × 100%.

Fluorescence titration experiments

The affinities of cap analogues for eIF4E was studied by time-synchronized titration method as described earlier (43). Fluorescence data were collected using an LS-55 spectrofluorometer (Perkin-Elmer Co.) and quartz cuvette (Hellma) with optical path length of 4 mm for absorption and 10 mm for emission. The experiments were performed at 20°C either in 50 mM HEPES/KOH buffer pH 7.20 containing 100 mM KCl, 0.5 mM EDTA and 1 mM DTT. Titration measurements were carried out by adding 1 μl aliquots of tested ligand to 1400 μl solution of 0.1 μM eIF4E. eIF4E fluorescence was excited at 280 nm (slit 2.5 nm, auto cut-off filter) and monitored at 340 nm (slit 4 nm, 290 nm cut-off filter), respectively. Data correction for sample dilution and inner filter effect were applied. Association equilibrium constants (*K*_{AS}) were determined by fitting the theoretical dependence of fluorescence intensity in the function of total concentration of tested ligand, according to the equation described earlier (43). Each experiment was repeated from three to six times, the final association constants *K*_{AS} were calculated as weighted average, with the weights taken from reciprocal standard deviations squared. Data were analyzed using Origin 6.0 software.

Inhibition of translation assays

Inhibition of cap-dependent translation in RRL (Flexi Rabbit Reticulocyte Lysate, Promega) by cap analogues, analysis of their stability in RRL and calculation of IC₅₀ values were performed as described previously. Briefly, the *in vitro* translation reaction was performed in 12.5 μl volume for 60 min at 30°C, in conditions determined for cap-dependent translation. The reaction mixture was pre-incubated for 60 min at 30°C prior to addition of dinucleotide cap analogue (inhibitor) and m₂^{7,3'-O}GpppG-capped luciferase mRNA to start the translation reaction. To analyse stability of studied cap analogues in rabbit reticulocyte lysate translation system, each cap analogue was incubated in a translation mixture for 60 min at 30°C and then luciferase mRNA was

added to start translation. Reactions were stopped by chilling on ice and the luciferase activity was measured in a luminometer (Glomax, Promega).

Translation efficiency in RRL system

Capped, polyadenylated luciferase mRNAs were synthesized *in vitro* on a dsDNA template (amplified by PCR reaction) that contained: SP6 promoter sequence of DNA-dependent RNA polymerase, 5'-UTR sequence of rabbit β -globin, the entire firefly luciferase ORF and a string of 31 adenosines. A typical *in vitro* transcription reaction mixture (40 μ l) contained: SP6 transcription buffer (ThermoFisher Scientific), 0.7 μ g of DNA template, 1 U/ μ l RiboLock Ribonuclease Inhibitor (ThermoFisher Scientific), 0.5 mM ATP/CTP/UTP and 0.1 mM GTP and 0.5 mM dinucleotide cap analogue (molar ratio cap analog:GTP 5:1). The reaction mixture was preincubated at 37°C for 5 min before addition of SP6 RNA polymerase (Fermentas) to final concentration 1 U/ μ l and reaction was continued for 45 min at 37°C. After incubation, reaction mixtures were treated with DNase RQ1 (Promega), in transcription buffer, for 20 min at 37°C at concentration 1 U per 1 μ g of template DNA. RNA transcripts were purified using NucAway Spin Columns (Ambion), integrity of transcripts was checked on a non-denaturing 1% agarose gel and concentrations were determined spectrophotometrically. A translation reaction in RRL was performed in 10 μ l volume for 60 min at 30°C, in conditions determined for cap-dependent translation. A typical reaction mixture contained: 40% RRL lysate, mixture of amino acids (0.01 mM), MgCl₂ (1.2 mM), potassium acetate (170 mM) and 5'-capped mRNA. Four different concentrations of each analysed transcript were tested in *in vitro* translation reaction. Activity of synthesized luciferase was measured in a luminometer.

In vitro RNA decapping assay with hDcp2

RNAs initiated with cap analogues were synthesized by *in vitro* transcription with SP6 polymerase and were generated on template of annealed oligonucleotides (ATACGATTTAGGTGACACTATAGAAGAAGC GGGCATGCGGCCAGCCATAGCCGATCA and TGATCGGCTATGGCTGGCCGCATGCCCGCTTCTTCTATAGTGTCACCTAAATCGTAT), which contain SP6 promoter sequence (ATTTAGGTGACACTATAGA) and encodes modified 35-nt sequence (GAAGAAGCGG GCATGCGGCCAGCCATAGCCGATCA) (44). Typical *in vitro* transcription reaction (20 μ l) was incubated in 40°C for 3 h and contained: RNA Pol Buffer (New England Biolabs), 1 U/ μ l SP6 polymerase, 1 U/ μ l RiboLock RNase Inhibitor, 0.5 mM ATP/CTP/UTP, 0.125 mM GTP, 1.25 mM cap analogue and 0.1 μ M annealed oligonucleotides as a template. To prepare uncapped RNAs, *in vitro* transcription reaction was performed as before, but with 0.5 mM GTP. Following 3 h incubation, 1 U/ μ l DNase I (ThermoFisher Scientific) was added and incubation was continued for 30 min at 37°C, after that EDTA was added to 25 μ M final concentration. RNAs were purified using RNA Clean & Concentrator-25 (Zymo Research) and their quality was checked on 15% acrylamide/7 M urea

1× TBE gels, whereas concentrations were determined spectrophotometrically.

Moreover, to obtain homogenous 3' end of synthesized RNAs, obtained 35-nt long transcripts (1 μ M) (capped RNAs were 36-nt long) were incubated with 1 μ M DNazyme 10–23 (TGATCGGCTAGGCTAGCTACAA CGAGGCTGGCCGC) in 50 mM MgCl₂ and 50 mM Tris–HCl pH 8.0 for 1 h at 37°C (44), what allow to produce a 3' homogenous 25-nt RNAs (capped RNAs were 26-nt long). Prepared transcripts were purified with RNA Clean & Concentrator-25 (Zymo Research) and DNase on-column. Their quality and concentration were checked as above.

In vitro decapping activity was measured with obtained transcripts after DNazyme 10–23 treatment. 100 ng of capped RNAs were subjected to digestion with 630 nM hDcp2 in decapping buffer (50 mM Tris–HCl pH 8.0, 50 mM NH₄Cl, 0.01% NP-40, 1 mM DTT, 5 mM MgCl₂ and 2 mM MnCl₂). Reactions were performed at 37°C for the indicated times and terminated by adding equal volume of loading dye (5 M urea, 44% formamide, 20 mM EDTA, 0.03% bromophenol blue, 0.03% xylene cyanol). RNAs after hDcp2 treatment were resolved electrophoretically on denaturing 15% acrylamide / 7 M urea 1× TBE gel and were stained with SYBR Gold (Invitrogen) and visualized using a Typhoon FLA 9500 (GE Healthcare).

Cell culture and *in vivo* measurements of translation efficiency

mRNAs encoding firefly luciferase for measurement of translational efficiency in HeLa cells were synthesized by *in vitro* transcription with SP6 polymerase using pJET_luc_128A plasmid digested with AarI (ThermoFisher Scientific) as a template. This plasmid was obtained by cloning sequence encoding firefly luciferase, two repeats of β -globin 3'UTR and 128 adenines from hRLuc-pRNA2(A)128 plasmid (45) into pJET1.2 vector (ThermoFisher Scientific). Typical *in vitro* transcription reaction (20 μ l) was incubated in 40°C for 3 h and contained: RNA Pol Buffer, 1 U/ μ l SP6 polymerase, 1 U/ μ l RiboLock RNase Inhibitor, 0.5 mM ATP/CTP/UTP, 0.125 mM GTP, 1.25 mM cap analogue and 0.1 μ g of digested plasmid as a template. Following 3 h incubation, 1 U/ μ l DNase I (ThermoFisher Scientific) was added and incubation was continued for 30 min at 37°C, after that EDTA was added to 25 μ M final concentration. Obtained mRNAs were purified with NucleoSpin RNA Clean-up XS (Macherey-Nagel) and their quality was checked on native 1.2% 1× TBE agarose gel, whereas concentrations were determined spectrophotometrically.

Human cervical carcinoma HeLa cells were grown in DMEM (Gibco) (with 2 mM L-glutamine (Gibco)) supplemented with 10% FBS (Sigma-Aldrich) and 1% penicillin/streptomycin (Gibco) at 5% CO₂ and 37°C. In a typical experiment 24 h before transfection, 10⁴ cells were seeded in 100 μ l medium without antibiotics per well of 96-well plate. Cells in each well were transfected for 1 h using 0.3 μ l Lipofectamine MessengerMAX Transfection Reagent (Invitrogen), 0.1 μ g mRNA and 10 μ l Opti-MEM (Gibco). After transfection, cells were washed with

PBS and supplemented with fresh medium without antibiotics, and grown for the indicated times. Cell lysis was performed using Luciferase Assay System (Promega) and bioluminescence flux was measured with the Synergy H1 microplate reader (BioTek). Obtained firefly luminescence was depicted as a function of time. Total protein expression was calculated as integral of the line segments connecting obtained data points for firefly luminescence.

Crystallography

Murine eukaryotic translation initiation factor 4E (eIF4E, residues 28–217) was expressed and purified as described previously (42) with an additional gel filtration purification step. The protein was concentrated to 4.75 mg/ml (Amicon 10 000 molecular weight Ultra Centrifugal Filter Device) in a gel filtration buffer (20 mM HEPES pH 7.2, 100 mM KCl, 0.5 mM EDTA, 2 mM DTT) and incubated with 0.5 mM cap analogues at room temperature for 15 min. Thin plate-like crystals were obtained using hanging drop vapor diffusion method at 18°C. Diffraction-quality crystals were formed in 13% PEG 5000 monomethyl ether, 0.1 M Tris-HCl pH 8.0 solution for eIF4E-m⁷GppppG complex and in 15% PEG 3350, 2% 1,4-dioxane, 0.1 M Tris-HCl pH 8.0 for eIF4E-m^{7,2'}O-GppCCl₂ppG within 1 day. Harvested crystals were transferred to the cryoprotectant solution (reservoir solution and glycerol 2:1 v/v) and flash frozen in liquid nitrogen. The X-Ray diffraction data sets were collected at 100 K at Bessy II (Helmholtz-Zentrum Berlin, Germany) Beamline 14.1 using a Dectris PILATUS detector and processed using XDS (46) with XDSAPP GUI (47). Structures were solved by Molecular Replacement using Phaser (48) and chain B of eIF4E-m⁷GppppG complex structure (PDB id: 1L8B) as a search model. Ligand dictionaries were generated using ProDRG (49) and JLigand (50). The model building and ligand fitting was performed in Coot (51), and the structures were refined using phenix.refine (52). The structures contain four copies of the protein in the asymmetric unit (chains A-D). High R-factor values result from significant disorder of two outermost protein molecules (chain C and D) as indicated by the wwPDB Validation report. Nonetheless, the electron density maps are very well defined for the majority of chain A and chain B residues and for the cores of chain C and D (Supplementary Figure S10). Data collection and refinement statistics are summarized in Supplementary Table S4.

¹⁹F NMR binding assays

Decoupled ¹⁹F{³¹P} NMR experiments were recorded using a Bruker AVIII 600 with BB-F/¹H Prodigy N₂ cryoprobe operating at 298 K using 5 mm diameter NMR tubes (Norell). ¹⁹F 90° pulse lengths were 15 μs and spectra were typically obtained using 128 scans for displacement experiments and a recovery delay of 2 s. Data were processed with 5 Hz Lorentzian line broadening using TopSpin 3.1 software (Bruker) and were referenced to the internal trifluoroacetic acid (TFA) standard (0.025 mM, −75.45 ppm). Samples typically contained 0.015 mM eIF4E and 0.025 mM m⁷GppCF₂ppG in HEPES (50 mM, pH 7.2) containing 100 mM KCl, 0.5 mM EDTA, 1 mM

DTT and 10% D₂O. Increasing amounts of displacing ligand (m⁷GppCCl₂p and m⁷GppCCl₂ppG) were added from stock solutions. The protein–ligand complex concentration [PL], which is equal to the concentration of m⁷GppCF₂ppG displaced from the protein, was then plotted against ligand concentration (*L*₀). The apparent association constant values *K*_{app} (defined as the inverse concentration of the free ligand (1/*L*) when 50% of the protein is bound to the ligand in the presence of the reporter ligand) were determined by fitting the experimental points to a theoretical curve [*PL*] = *P*₀*L*₀/(1/*K*_{app} + *L*₀).

The actual association constants were calculated using equations derived from equations previously described by Nikolovska-Coleska *et al.* (53) and Leung *et al.* (54). When concentration of the reporter ligand *R*₀ and its association constant (*K*_{rep}) are known, the correlation between apparent association constant *K*_{app} of the ligand and the actual association constant *K*_{AS} is given by equation: *K*_{AS} = *K*_{app}([*R*₅₀]*K*_{rep} + [*P*]*K*_{rep} + 1), where [*R*₅₀] is the free reporter ligand concentration when 50% of the ligand is displaced from the enzyme and [*P*] is the free enzyme concentration in the presence of reporter ligand. [*R*₅₀] is described as: [*R*₅₀] = *R*₀ − 0.5(*P*₀ − [*P*]), where *P*₀ is the initial (i.e. total) concentration of enzyme and *R*₀ is the total concentration of the reporter ligand. [*P*] is given by equation: [*P*] = −0.5(1/*K*_{rep} + *R*₀ − *P*₀) + 0.5((1/*K*_{rep} + *R*₀ − *P*₀)² + 4*P*₀/*K*_{rep})^{0.5}. For calculations following values were used: *P*₀ = 15 μM, *R*₀ = 25 μM, *K*_{rep} = 57.6 μM^{−1}.

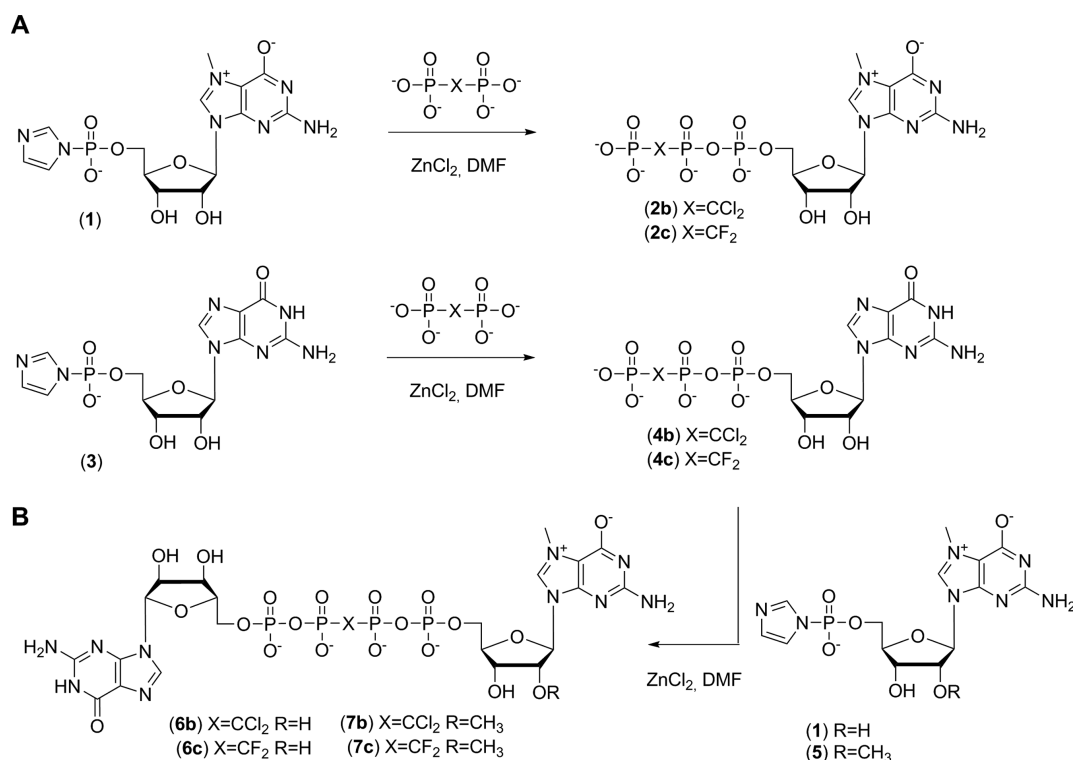
Monitoring enzymatic reactions by ¹⁹F NMR

The reactions were run in standard 5 mm NMR tubes and contained 2 mM m⁷GppCF₂ppG (6c) in 600 μl of DcpS buffer (50 mM Tris-HCl pH 7.9 containing 150 mM NaCl, 2 mM DTT and 15% D₂O). Just before placing in the NMR apparatus 20 μl of 5 μM hDcpS enzyme were added to the samples (to a final concentration of 160 nM). The reactions were monitored at 30°C using a standard ¹⁹F NMR pulse sequence (16 transients) in 2.7 min intervals. The spectra were recorded on 400 MHz spectrometer using 5 mm 4NUC probe. The resonances were assigned based on reference ¹⁹F NMR spectra of pure substrate (m⁷GppCF₂ppG, 6c) and product (GppCF₂p, 4c), respectively.

RESULTS

Synthesis

The mononucleotide cap analogues 2b–c were synthesized by the coupling of an appropriate triethylammonium dihalomethylenbisphosphonate with an imidazole derivative of a 7-methylguanosine monophosphate 1 in DMF in the presence of ZnCl₂ (40,55). Similarly, coupling of an appropriate dihalomethylenbisphosphonate (pCF₂p or pCCl₂p) with an imidazole derivative of a guanosine monophosphate 3 yielded modified guanosine triphosphates 4b–c, which were then further coupled with an imidazole derivative of either 7-methyl (1) or 7,2'-*O*-dimethylguanosine monophosphate (5) to yield dinucleotide cap analogues 6b–c and 7b–c, respectively (Scheme 1).



Scheme 1. Synthesis of dihalogenated cap analogues.

Biophysical and spectroscopic characterization

To assess the influence of various bridging oxygen substitutions on the electronic properties of the tri- or tetraphosphate bridge within the cap structure, we first compared the ^{31}P NMR chemical shifts (δ_{P}) for cap analogues **2a–d** and **6a–d** (Table 1, values measured in D_2O). The δ_{P} values for difluoromethylene, followed by dichloromethylene-containing caps were closer to the δ_{P} values of the pyrophosphate-containing analogues than to those of methylene-containing caps. This observation confirmed our suggestion that, the introduction of halogen substituents at the methylene moiety might lead to closer mimics of pyrophosphate. Since the chemical shifts of ionizable groups may significantly depend on the pH, we also investigated the pH dependence of δ_{P} for mononucleotides **2a–d** (Supplementary Figure S1). The chemical shifts for β and γ phosphates were highly dependent on the pH in the range from 5 to 9, but the general tendency observed for the samples prepared in D_2O (initial measurements of ^{31}P NMR spectra) was preserved. Furthermore, this experiment enabled the determination of $\text{p}K_{\text{a}}^4$ values for analogues **2a–d** (Table 1, Supplementary Table S1). The $\text{p}K_{\text{a}}$ value was the highest for methylene analogue **2a** ($\text{p}K_{\text{a}}^4 = 8.6$) and decreased with the addition of chlorine and fluorine substituents ($\text{p}K_{\text{a}}^4 = 7.4$ and 6.4 for **2b** and **2c**, respectively). The unmodified analogue **2d** was characterized by a $\text{p}K_{\text{a}}^4$ value of 6.9 , placing it between dichloromethylene- and difluoromethylene analogues **2b** and **2c**. These data were in good agreement with the previously reported values for adenosine 5'-triphosphate analogues (**14**) (Supplementary Table S2, Figure S3).

Binding to eIF4E

Initiation of translation is the rate limiting step of protein biosynthesis and involves binding of the mRNA cap by the eIF4F pre-initiation complex. Specifically, the cap structure is recognized by eIF4E, which is a part of the eIF4F assembly, therefore high affinity for eIF4E is a desirable feature that could indicate an increase in translational potency of mRNAs with chemically modified cap analogues at their 5' ends. On the other hand, eIF4E is often overexpressed in cancer cells and is a target of interest in anti-cancer therapy (**6–8,56**), thus high-affinity ligand binding to eIF4E is also required for obtaining small molecule inhibitors of translation. Targeting eIF4E with cap analogues is one of the potential strategies to counteract its overexpression in cancer cells. Therefore, eIF4E-cap interaction is one of the most important properties determined for novel cap analogues. The dihalomethylene cap analogues (**2b–c**, **6b–c** and **7b–c**) were evaluated as eIF4E binders by determining equilibrium association constants (K_{AS}) using a fluorescence titration method (Table 2, Supplementary Figure S3) (**43**). In the case of mononucleotide triphosphates (**2a–d**), the dihalomethylene cap analogues **2b** and **2c** were characterized by K_{AS} values similar and 1.5-fold higher compared to the unmodified parent analogue **2d** (K_{AS} of 188.1 and $115 \mu\text{M}^{-1}$ for **2b** and **2c**, respectively, and $108.7 \mu\text{M}^{-1}$ for **2d**). In contrast, the methylene analogue **2a** exhibited a K_{AS} 6-fold lower than **2d** ($K_{\text{AS}} = 19.5 \mu\text{M}^{-1}$). The binding affinities for the dinucleotide tetraphosphates **6a–d** and **7a–d** revealed the same general tendency however, with smaller differences between the methylene and dihalogenomethylene modifications. As in the case of mononucleotides, the high-

Table 1. ^{31}P NMR chemical shifts and $\text{p}K_{\text{a}}^4$ values for modified cap analogues

Cap analogue	^{31}P NMR chemical shifts— δ_{P} [ppm]				$\text{p}K_{\text{a}}^4$
	$\text{P}\alpha$	$\text{P}\beta$	$\text{P}\gamma$	$\text{P}\delta$	
$\text{m}^7\text{GppCH}_2\text{p}$ (2a)	−10.16	10.21	15.03	—	8.63 ± 0.01
$\text{m}^7\text{GppCCl}_2\text{p}$ (2b)	−10.58	0.88	7.90	—	7.32 ± 0.07
$\text{m}^7\text{GppCF}_2\text{p}$ (2c)	−10.90	−3.51	3.49	—	6.28 ± 0.07
m^7Gppp (2d)	−10.56	−22.22	−9.83	—	6.56 ± 0.03
$\text{m}^7\text{GppCH}_2\text{ppG}$ (6a)	−10.76	7.75	7.75	−10.76	—
$\text{m}^7\text{GppCCl}_2\text{ppG}$ (6b)	−10.81	−1.41	−1.41	−10.81	—
$\text{m}^7\text{GppCF}_2\text{ppG}$ (6c)	−11.08	−6.37	−6.37	−11.08	—
m^7GppppG (6d)	−10.47	−22.04	−22.04	−10.47	—

Table 2. Equilibrium association constants (K_{AS}) for cap analogue—eIF4E complexes as measured by fluorescence quenching titration experiments

X	K_{AS} [μM^{-1}]		
	m^7GppXp	$\text{m}^7\text{GppXppG}$	$\text{m}_2^{7,2'-\text{O}}\text{GppXppG}$
O	$108.7 \pm 4.0^{\text{a}}$	$102.8 \pm 4.4^{\text{a}}$	$99.8 \pm 6.0^{\text{b}}$
CH_2	19.5 ± 1.4	$48.6 \pm 2.1^{\text{c}}$	$44.0 \pm 3.2^{\text{c}}$
CCl_2	188.1 ± 7.4	77.9 ± 1.7	82.8 ± 1.1
CF_2	115.2 ± 5.8	57.6 ± 0.8	50.0 ± 1.8

^aData from Niedzwiedzka *et al.* (26).^bData from Jemielity *et al.* (22).^cData from Rydzik *et al.* (20).

Measurements were carried out in the following conditions: 50 mM HEPES/ KOH pH = 7.2, 0.1 M KCl, 0.5 mM EDTA and 1 mM DTT.

est affinity among the phosphate-modified dinucleotides was observed for the dichloromethylene compounds **6b** and **7b**, which had K_{AS} values only slightly lower than those of the phosphate-unmodified parent dinucleotides **6d** and **7d** (K_{AS} of 77.9 and 82.8 μM^{-1} for **6b** and **7b**, respectively; 102.8 μM^{-1} and 99.8 μM^{-1} for **6d** and **7d**, respectively). The difluoromethylene analogues **6c** and **7c** were weaker binders (K_{AS} of 57.6 and 50.0 μM^{-1} for **6c** and **7c**, respectively), with K_{AS} values almost 2-fold lower compared to those of the unmodified parent dinucleotides (**6d** and **7d**, respectively) and only slightly higher than the affinities of the methylene analogues **6a** and **7a** (K_{AS} of 48.6 μM^{-1} and 44.0 μM^{-1} for **6a** and **7a**, respectively).

Crystallography

To further investigate the role of a pCCl_2p moiety in the stabilization of cap-eIF4E interactions, we obtained co-crystal structures of a murine eIF4E (residues 28–217) in a complex with the dichloromethylene analogue **7b** ($\text{m}_2^{7,2'-\text{O}}\text{GppCCl}_2\text{ppG}$) (PDB id: 5J5Y) and a cap analogue **6d** unmodified in the tetraphosphate bridge (m^7GppppG) (PDB id: 5J5O) determined to 1.75 Å and 1.87 Å resolution, respectively. In both complexes the 7-methylguanine is stacked between two tryptophan sidechains (Trp56 and Trp102) and hydrogen bonded to the carboxylic group of Glu103. The ribose ring adopts a C3'-endo conformation so that the phosphorus atoms of the two downstream phosphates (δ and γ for tetraphosphates) lay nearly coplanar with the 7-methylguanine, participating in ionic interactions with the positively charged side chains of Lys162 and

Arg157 and an extensive net of hydrogen bonds mediated by water molecules (Figure 2A and B).

The structure of eIF4E in a complex with m^7GppppG (**6d**) reveals a very similar ligand binding mode as in the previously reported eIF4E- m^7GpppG complex (PDB id: 1L8B, overlay in Figure 2C) (43). For **6d**, similar to m^7GpppG , the oligophosphate bridge continues in a perpendicular direction toward the C-terminal loop, resulting in strong ionic contacts between a β -phosphate and Lys162 as well as the formation of several hydrogen bonds with water molecules. An additional phosphate in **6d** (α -phosphate) forms an ionic contact with Lys159, which is probably responsible for the increase of the association constant, compared to m^7GpppG .

On the other hand, in the structure of eIF4E in complex with $\text{m}_2^{7,2'-\text{O}}\text{GppCCl}_2\text{ppG}$ (**7b**), the tetraphosphate bridge of **7b** adopts an essentially different conformation (Figure 2D). The conformation of analogue **7b** is likely forced by steric hindrance between the chlorine atom and C5' of 7-methylguanosine. To avoid a clash, the bridging β/γ - CCl_2 -carbon atom of **7b** is located approximately coplanar with γ and δ phosphates and the β -phosphate continues outside of the binding pocket, impairing ionic interactions with Lys162. However, the β -phosphate moiety forms ionic contact with Lys159, thus compensating the energetic loss to some extent. Finally, in all the **6d**, **7b**, and m^7GpppG co-crystal structures the second nucleoside is disordered, so that the electron density was not defined for that part of the ligands, suggesting that they do not form any specific and strong interactions with the protein.

Susceptibility to enzymatic hydrolysis by hDcpS

The utility of cap analogues for studies in complex biological mixtures and *in vivo* is quite often hampered by their poor stability arising from hydrolysis by cellular pyrophosphatases (38). In humans, short capped RNA oligonucleotides and mono- and dinucleotide caps are targets for a human decapping scavenger enzyme (hDcpS), which is a member of HIT family pyrophosphatases (57) and cleaves the triphosphate chain of a dinucleotide cap between the γ and β phosphates (Supplementary Figure S4) (58). The influence of a dihalomethylene moiety on the enzymatic susceptibility of analogues **2b,c**, **6b,c** and **7b,c** to hDcpS was studied using an HPLC assay (37,38,59). The enzymatic reaction progress was analyzed at four different time points (15, 30, 60 and 120 min). The previously studied unmodified parent compounds and their corresponding methylene

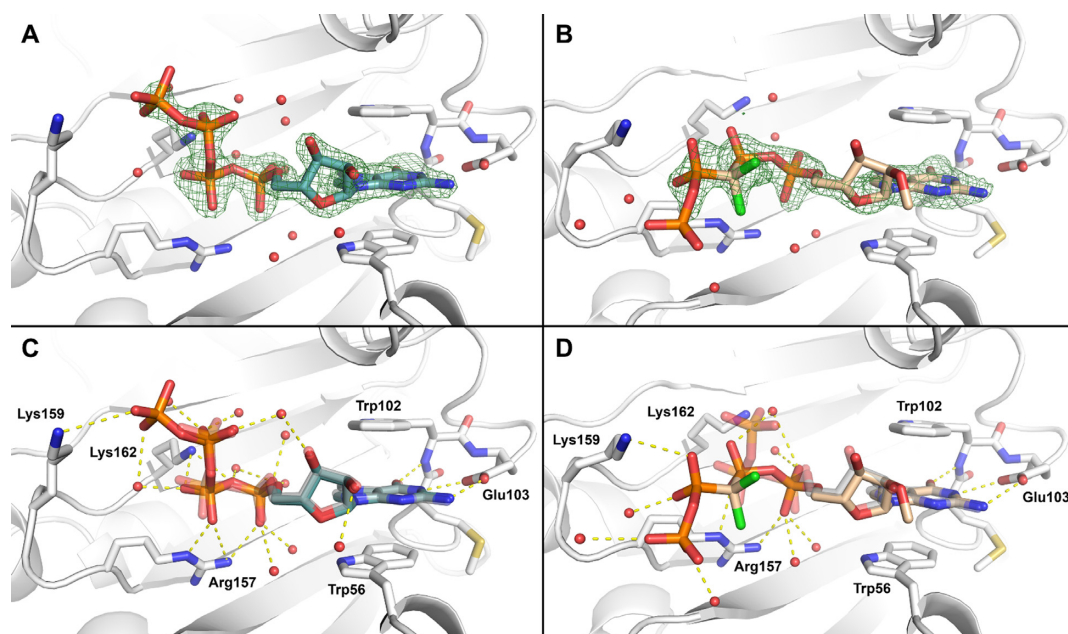


Figure 2. (A) Close-up view of the ligand binding in the crystal structure of eIF4E in complex with m^7 GppppG (**6d**) (PDB id: 5J5O, including simulated annealing omit $F_o - F_c$ electron density map contoured at 3σ). (B) Close-up view of the ligand binding in the crystal structure of eIF4E in complex with $m_2^{7,2'O}$ GppCCl₂ppG (**7b**) (PDB id: 5J5Y, including a simulated annealing omit $F_o - F_c$ electron density map contoured at 3σ). (C) Superposition of crystal structures of eIF4E in complex with m^7 GppppG (**6d**) (PDB id: 5J5O) and m^7 GpppG (PDB id: 1L8B) reveal similar binding modes for both ligands. (D) Superposition of crystal structures of eIF4E in complex with $m_2^{7,2'O}$ GppCCl₂ppG (**7b**) (PDB id: 5J5Y) and m^7 GpppG (PDB id: 1L8B) reveal different conformation of the tetraphosphate bridge of analogue **7b** in comparison to m^7 GpppG.

Table 3. Enzymatic hydrolysis of cap analogues by hDcpS

X	% hydrolysis after 1 h incubation with hDcpS ^b		
	m^7 GppXp	m^7 GppXppG	$m_2^{7,2'O}$ GppXppG
O	43.9 ± 3.5	90.0 ± 2.3	–
CH ₂ ^a	0	0	0
CCl ₂	1.1 ± 0.3	0	0
CF ₂	6.9 ± 0.0	50.1 ± 1.8	8.1 ± 0.7

^aData from Rydzik *et al.* (20).

^bReactions were carried out using 0.04 mM cap analogue and 62.5 nM hDcpS in 50 mM TRIS buffer pH = 7.5 containing 0.2 M KCl, 0.5 mM EDTA and 1.2 mM DTT.

analogues were included in the assay as references. The results after 1 h are shown in Table 3, whereas data for all the time points are summarized in the Supporting Information (Supplementary Figure S5, Table S3).

In agreement with previous reports (37,38,59), we found that dinucleotide analogues are generally more susceptible to hydrolysis by hDcpS than mononucleotides. While the unmodified analogue 44% of m^7 Gppp (**2d**) was hydrolyzed after 1 h incubation with hDcpS, the dinucleotide cap m^7 GppppG (**6d**) was hydrolyzed to ~90%. Under the same conditions, the modified mononucleotides were hydrolyzed significantly slower: difluoromethylene analogue (**2c**) was hydrolyzed in 7%, whereas dichloromethylene (**2b**) and methylene (**2a**) analogues were virtually resistant toward enzymatic hydrolysis (Table 3). In the dinucleotide series, the methylene (**6a**) and dichloromethylene (**6b**) analogues were also resistant to hDcpS, whereas the difluo-

romethylene compound (**6c**) was a fairly good substrate for hDcpS (approximately 50% cleavage after 1 h).

The ARCA compounds, i.e. those bearing an additional methyl group in the 2'-O position of the ribose ring, are known to be less susceptible to hDcpS than their unmethylated counterparts (35–37). Accordingly, compound **7c** was hydrolyzed slower than **6c** (8% and 50%, after 1 h, respectively).

Susceptibility to decapping enzyme hDcp2

Decapping is the first irreversible event in 5'-to-3' mRNA degradation pathway. mRNA decapping is executed by Dcp1-Dcp2 complex, in which Dcp2 is the catalytically active subunit and a member of Nudix (nucleoside diphosphate linked to another moiety X) hydrolase superfamily of proteins. In contrast to DcpS, hDcp2 catalyzes cleavage between α and β phosphates in the 5'-5'-triphosphate chain, releasing 7-methylguanosine diphosphate and 5' monophosphorylated mRNA (Supplementary Figure S4) (60). The decapped mRNA is no longer available for translational machinery and is subjected to further degradation by Xrn1, main cytoplasmic 5'-3' exonuclease (3). Increased resistance of mRNA cap to hDcp2 has been shown to extend mRNA half-life in cells, thereby prolonging and increasing overall protein expression. *In vitro* susceptibility to decapping of transcripts capped with analogs **7a-d** was assayed by incubation of short capped transcripts with hDcp2, followed by resolution of the reaction mixtures on high resolution polyacrylamide gel in order to separate capped and decapped RNAs (Supplementary Figure S6). Gels were stained with fluorescent dye, visualized and in-

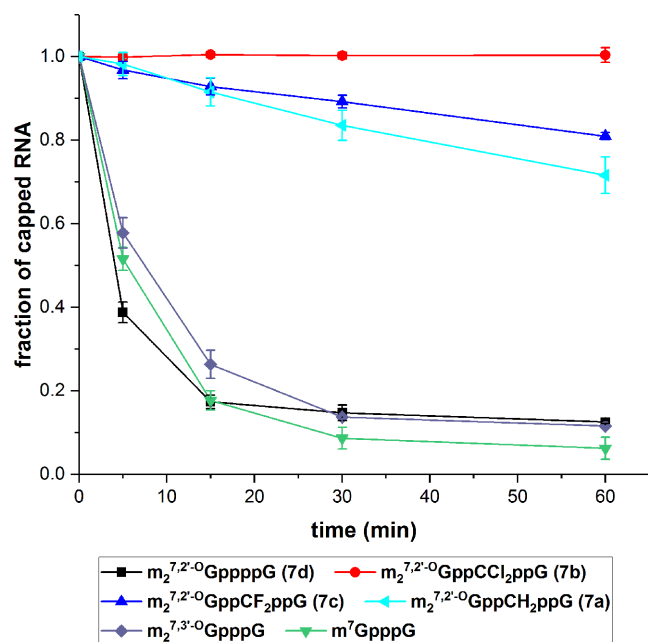


Figure 3. Susceptibility of differently capped RNAs to hDcp2. The data represent quantified results from duplicate experiments (gels from the decapping assay are shown in Supplementary Figure S6). Fraction of capped RNA was calculated as a ratio of capped RNA band intensity to total RNA at a given time. All data were normalized to time 0'.

Table 4. Enzymatic hydrolysis of capped RNAs by hDcp2

Cap analogue	Decapping susceptibility (%) ^{a,b}
$m_2^{7,2'-O}$ GppppG (7d)	83 ± 2
$m_2^{7,2'-O}$ GppCH ₂ ppG (7a)	8 ± 3
$m_2^{7,2'-O}$ GppCCl ₂ ppG (7b)	0 ± 1
$m_2^{7,2'-O}$ GppCF ₂ ppG (7c)	7 ± 2
$m_2^{7,3'-O}$ GppppG	74 ± 3
m^7 GppppG	82 ± 2

^a% of RNA decapping after 15 min incubation with hDcp2.

^bReactions were carried out using 100 ng of capped RNA and 630 nM hDcp2 50 mM Tris-HCl pH 8.0, 50 mM NH₄Cl, 0.01% NP-40, 1 mM DTT, 5 mM MgCl₂ and 2 mM MnCl₂.

tensity of bands corresponding to both versions of RNA was determined densitometrically. Figure 3 depicts the fraction of capped RNA remaining at various timepoints, while Table 4 shows RNA decapping susceptibilities, defined as a percentage of decapped RNA to total RNA at a time-point 15 min. As expected, the presence of methylene or dihalomethylene moiety in the cap's tetraphosphate chain stabilized the transcripts against Dcp2 (Table 4, Figure 3). The decapping susceptibilities for RNA capped with compounds **7a**, **7b** and **7c** were 8 ± 3, 0 ± 1 and 7 ± 2, respectively, compared to 74 ± 3, and 83 ± 2 for reference analogs $m_2^{7,3'-O}$ GppppG and $m_2^{7,2'-O}$ GppppG (**7d**), respectively. In particular, RNA capped with the dichloro-containing analogue **7b** was fully resistant against hDcp2 under the assay conditions.

Inhibition of translation in RRL system

Following the promising results from eIF4E binding and enzymatic stability experiments (susceptibility to hDcpS and to hDcp2) we investigated the modified cap analogues as inhibitors of cap-dependent translation. The IC₅₀ values for cap analogues **2a–c**, **6a–c** and **7a–c** were determined in the rabbit reticulocyte lysate (RRL) system utilizing a luciferase reporter gene based assay (38) (Table 5). Two set of experiments were conducted. In the first, the cap analogue of interest and a reporter mRNA were added simultaneously to the RRL system and the mixture was incubated for 60 min at 30°C prior to the measurement (set A). In the second, the cap analogue was preincubated in the RRL system for 60 min prior to the addition of a reporter mRNA and then mixture was incubated for a further 60 min at 30°C before the measurement (set B) (Supplementary Figures S7 and S8). The second set of experiments took into account enzymatic stability of the studied compounds through their extended exposure to cellular lysate of reticulocytes (38). The pCH₂p analogues (**2a**, **6a** and **7a**) were characterized by the highest IC₅₀ values, which is in agreement with previous findings (61) and likely results from their low binding affinities to eIF4E. A clear improvement in the IC₅₀ values was observed in the case of pCCl₂p analogues compared to their pCH₂p and unmodified counterparts. Consistent with the highest binding affinities for eIF4E, the pCCl₂p-containing caps (**2b**, **6b** and **7b**) were characterized by the lowest IC₅₀ values. Unlike analogues unmodified in the phosphate bridge (**2d**, **6d** and **7d**), the pCH₂p and pCCl₂p analogues (**2a–b**, **6a–b** and **7a–b**) were relatively stable in RRL since they retained a similar activity both with and without pre-incubation. In particular, the pCCl₂p analogues **2b** and **7b** were identified as potent inhibitors of translation in the RRL system (IC₅₀ of 0.97 and 0.95 μM for **2b** and **7b** respectively).

Synthesis and translation efficiency of 5'-capped mRNAs

Cap is an integral part of mRNA and therefore we were interested in evaluating how introduction of dichloro- and difluoromethylene modifications into phosphate chain would influence the efficiency of translation of mRNAs capped with such analogues. For these experiments, transcripts encoding firefly luciferase and capped with ARCA **7a–d** or a commercially available ARCA ($m_2^{7,3'-O}$ GppppG) were synthesized by *in vitro* transcription using SP6 polymerase. The translation efficiencies in rabbit reticulocyte lysate system (RRL) for differently capped RNAs were measured by luminometry after 1 h and referred to the control mRNA capped with m^7 GppppG (Table 6, Supplementary Figure S9). Additionally, the level of cap-independent translation was estimated using transcripts capped with the non-functional analogue AppppG. The translation efficiencies of $m_2^{7,3'-O}$ GppppG-capped mRNAs were 1.6-fold higher than that of m^7 GppppG-capped RNA, which is in agreement with previously published work and attributed to the “anti-reverse” properties of $m_2^{7,3'-O}$ GppppG (40). The unmodified tetraphosphate ARCA analogue **7d** had slightly higher translation efficiency than $m_2^{7,3'-O}$ GppppG, which also agrees with previous observations and has been explained by an increased affinity for eIF4E conferred by

Table 5. IC₅₀ values for the inhibition of translation in the rabbit reticulocyte lysate system by cap analogues

X	IC ₅₀ [μM]					
	m ⁷ GppXp		m ⁷ GppXppG		m ₂ ^{7,2'-O} GppXppG	
	Inhibition ^a	Stability ^a	Inhibition ^a	Stability ^a	Inhibition ^a	Stability ^a
O	3.52 ± 0.25	7.57 ± 0.27	5.0 ± 0.5 ^b	> 20 ^b	2.8 ± 0.2 ^b	4.2 ± 0.1 ^b
CH ₂	8.09 ± 1.18	9.87 ± 0.84	4.6 ± 0.6 ^b	3.8 ± 0.2 ^b	2.8 ± 0.2 ^b	2.9 ± 0.3 ^b
CCl ₂	0.97 ± 0.13	1.37 ± 0.01	1.34 ± 0.15	1.52 ± 0.10	0.95 ± 0.10	1.23 ± 0.11
CF ₂	1.81 ± 0.13	2.43 ± 0.07	2.95 ± 0.32	4.99 ± 0.41	2.16 ± 0.23	3.59 ± 0.28

^aSet A and B refer to the experiments conducted without (A) and with (B) cap analogue preincubation in RRL system.
^bData from Rydzik *et al.* (20).

Table 6. *In vitro* translation efficiency of mRNA capped with different cap analogues

Cap analogue	Relative translation efficiency
m ⁷ GpppG	1.00 ± 0.02
m ₂ ^{7,3'-O} GpppG	1.60 ± 0.16
m ₂ ^{7,2'-O} GppppG (7d)	1.77 ± 0.18
m ₂ ^{7,2'-O} GppCH ₂ ppG (7a)	1.39 ± 0.33
m ₂ ^{7,2'-O} GppCCl ₂ ppG (7b)	1.71 ± 0.25
m ₂ ^{7,2'-O} GppCF ₂ ppG (7c)	1.57 ± 0.10
ApppG	0.19 ± 0.10

the additional phosphate group (40,56). Despite higher affinity to eIF4E, transcripts capped with the pCH₂p analogue **7a** were translated less efficiently than mRNA capped with m₂^{7,3'-O}GpppG however, mRNAs capped with the dihalomethylene analogues **7b** and **7c** both had higher translational efficiencies than the methylene analogue **7a**. Notably, the pCCl₂p analogue **7b** outperformed other modified analogues and conferred an mRNA translational efficiency similar to that of the unmodified tetraphosphate **7d**.

Next, we investigated whether mRNAs capped with the dihalomethylene analogues **7b** and **7c** would yield more protein than transcript capped with analogue **7a** in a more complex system, i.e. living cells. Taking into account lower susceptibility to hDcp2 of transcripts capped with **7b** and **7c** compared to transcripts capped with **7d** (Table 4, Figure 3) we envisaged that mRNAs carrying analogues **7b** and **7c** could be more stable *in vivo* than transcripts capped with **7d**, thereby giving higher overall protein yield. Translation efficiencies were determined in HeLa cells transfected with equal amounts of RNA encoding firefly luciferase and capped with analogues **7a–d**. After cell lysis, luciferase activity was measured and plotted as a function of time (Figure 4A). Moreover, the relative total protein expression, defined as the integral under expression curve normalized to the expression of RNA capped with **7d**, was calculated for each transcript (Figure 4B). We found that the total protein expression was higher for mRNA capped with the pCCl₂p analogue **7b** than with unmodified tetraphosphate ARCA **7d** (relative total protein expression equal 1.18), which is expressed about two fold more efficiently than transcripts capped with analogues **7a** and **7c**.

Applications of fluorinated cap analogues in ¹⁹F NMR studies

¹⁹F NMR is gaining increasing attention as a useful tool for studying protein-ligand interactions (62–65). In partic-

ular, the virtual absence of fluorine in biological material allows the measurement of specific interactions between fluorinated reporter tags and proteins even in complex samples including cells (66,67). Therefore, we tested the fluorinated cap analogue **6c** as a reporter ligand in binding assays as well as an activity-based probe for monitoring enzymatic hydrolysis by ¹⁹F NMR.

eIF4E is overexpressed in many types of cancer and constitutes an important molecular target for anti-cancer therapy (6). Therefore, methods for studying binding to the eIF4E active site are of interest, in particular from the inhibitor discovery perspective. Having established that the difluoromethylene-containing cap analogues are good eIF4E binders, we decided to evaluate their use as reporter molecules in the ¹⁹F NMR binding assay. The assay is based on the initial binding of a fluorinated reporter molecule to eIF4E, which typically results in the significant broadening of the ¹⁹F NMR signal of a ligand owing to increased transverse relaxation rates. Subsequently, the reporter ligand is displaced from complex with eIF4E, which results in a recovery of the ¹⁹F signal of the unbound reporter (Figure 5A) (68). Here, we exemplify the method using the dinucleotide analogue **6c** (m⁷GppCF₂ppG), as it was characterized by a lower affinity for eIF4E in comparison to mononucleotide analogue **2c**. This might be of advantage in the displacement assays, especially when testing ligands with low binding affinities. In our case, the two pCCl₂p analogues **2b** and **6b**, which exhibit different affinities to eIF4E, were used as model ligands (Figure 5A). Using the ¹⁹F NMR observed method, we were able to determine apparent association constant values (*K*_{AS,app} = 0.164 and 0.017 μM⁻¹ for **2b** and **6b** respectively), which led to actual *K*_{AS} values of 166 and 17.2 μM⁻¹ for the respective analogues. This is in a good agreement with the data obtained from fluorescence titration experiments (188 and 78 μM⁻¹ for analogues **2b** and **6b** respectively, Table 2).

Another therapeutically relevant cap-binding protein is hDcpS, which was identified as a molecular target in spinal muscular atrophy (34,69). However, the same approach as used for eIF4E cannot be applied to search for hDcpS binders, since all difluoromethylene cap analogues are susceptible to degradation by hDcpS. Instead, we applied the cap analogue m⁷GppCF₂ppG (**6c**) as an activity-based probe to monitor DcpS-mediated hydrolysis leading to the production of m⁷GMP and GppCF₂p (**4c**) (Figure 5B). The fluorinated analogue **6c** was observed to be a relatively good

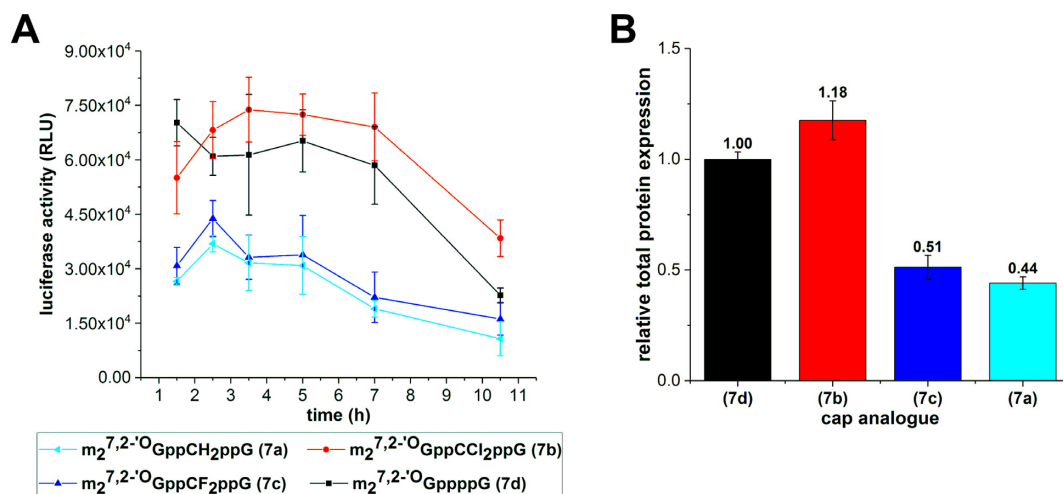


Figure 4. Expression of capped-mRNA in HeLa cell line. (A) Firefly luciferase activity depicted as function of time. (B) Total protein expression of firefly luciferase normalized to $m_2^{7,2'-O}GpppppG$ -mRNA. Values above each bar represent relative protein expression.

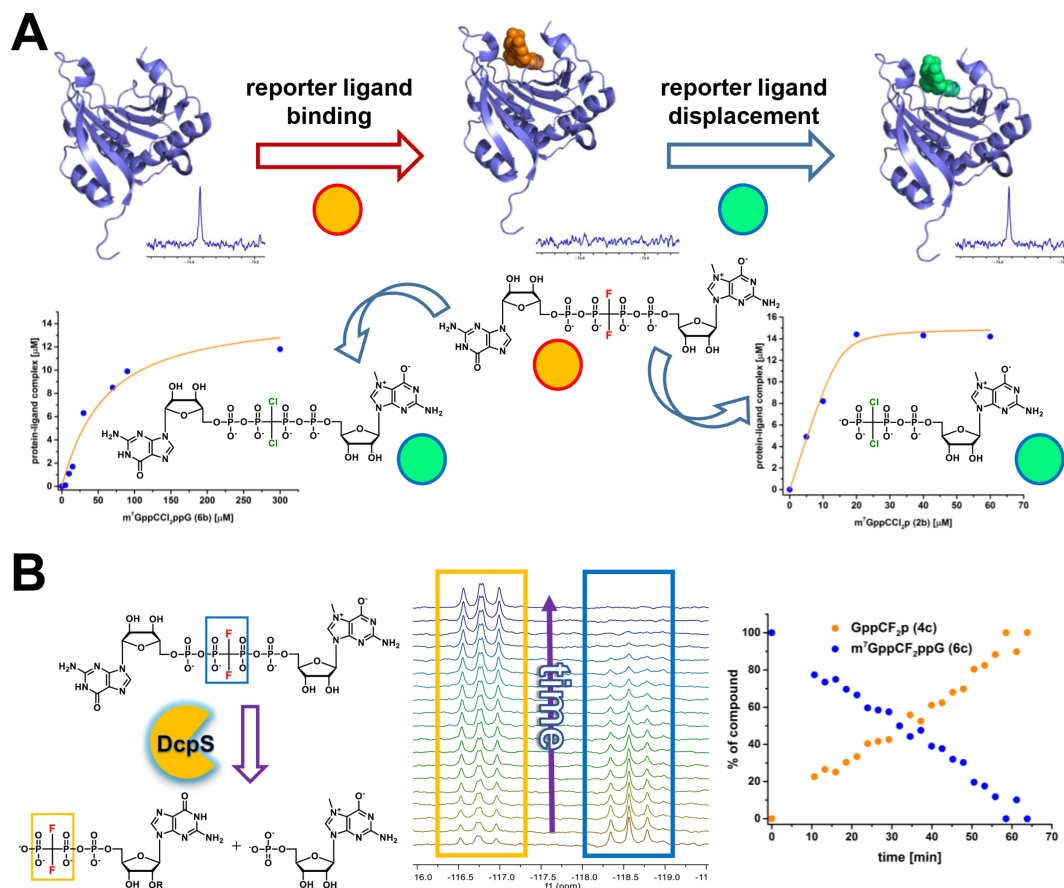


Figure 5. Applications of fluorinated cap analogues. (A) Basis of the displacement assay followed by the ¹⁹F NMR signal of the reporter molecule m^7GppCF_2ppG (6c). The displacement of 6c by $m^7GppCCl_2p$ (2b) and $m^7GppCCl_2ppG$ (6b) yields binding curves typical for strong and weaker binders, respectively. (B) Hydrolysis of m^7GppCF_2ppG (6c) by the DcpS enzyme followed by ¹⁹F NMR.

substrate for hDcpS and therefore might find use as a reporter ligand for hDcpS inhibition studies.

DISCUSSION

We described the synthesis and properties of novel mRNA 5'-cap analogues bearing the dichloromethylene- or difluoromethylenebisphosphonate moiety as a bridging modification of the oligophosphate chain. ^{31}P NMR and pK_a measurements confirmed that introduction of an electronegative substituent into the methylene moiety influenced the electronic properties of neighboring phosphates to more closely mimic the parent pyrophosphate containing cap structure.

High affinity of ligand binding to eIF4E is required for obtaining small molecule inhibitors of translation or, in the case of mRNA modification, high translational efficiencies. Therefore, eIF4E-cap interaction is one of the most important properties determined for novel cap analogues. Generally, the introduction of both pCCl_2p and pCF_2p moieties stabilized the cap-eIF4E complex compared to the pCH_2p -containing analogues, however, the effect was more pronounced for mononucleotides. The significantly lower affinity of $\text{m}^7\text{GppCH}_2\text{p}$ (**2a**) might be partially explained by a smaller negative net charge compared to other mononucleotides. It has been shown that electrostatic interactions between the negatively charged phosphate chain and basic amino acids in the cap-binding pocket play an important role in complex stabilization, and that the affinity of cap analogues for eIF4E increases with the increasing negative net charge of the polyphosphate chain (43,56). The pK_a value for the compound **2a** determined by ^{31}P NMR was above 8 whereas for the other analogues it was below 7.5. Therefore, at the pH of the binding experiment (pH 7.2) compound **2a** might have a notably smaller negative charge compared to the other mononucleotides. However, this observation does not account for the general stabilization of cap-eIF4E complexes observed for dichloromethylene analogues compared to methylene and difluoromethylene substitutions. This was observed both in the mono- and dinucleotides series, and despite the lower pK_a of pCF_2p analogue **2c** compared to pCCl_2p analogue **2b**, suggests that an additional stabilizing effect is provided exclusively by the pCCl_2p group.

To obtain a deeper insight into the interaction of chlorinated cap analogue with the eIF4E protein, we obtained crystal structures of $\text{m}^7\text{GppCCl}_2\text{ppG}$ (**6c**) and m^7GppppG (**6d**) in complex with eIF4E. Notably, the dichloromethylene moiety in analogue **6c** appears to alter the ligand binding mode compared to a cap analogue unmodified in the tetraphosphate bridge (**6d**). It indicates, that apart from the electronic effects, the geometry of a polyphosphate moiety might make a major contribution to the binding affinity.

The utility of cap analogues as potential inhibitors of eIF4E is also determined by their hydrolytic stability in a cell environment. We have evaluated the susceptibility of cap analogues **2a-d**, **6a-d** and **7a-d** to cap specific pyrophosphatase DcpS, which in human targets short capped RNA oligonucleotides and mono- and dinucleotide caps (57,58). In the experimental conditions, apart from the unmodified nucleotides, only difluoromethylene-containing

analogues were significantly susceptible to hDcpS-mediated hydrolysis. This indicates that the pCF_2p moiety is the closest mimic of a pyrophosphate in respect to recognition by hDcpS. This might result from the pCF_2p moiety being a better leaving group compared to pCH_2p , combined with its small size allowing the avoidance of steric hindrance in the cap binding pocket. Such steric hindrance might also be a reason for the resistance of the pCCl_2p -containing analogues toward hDcpS. This feature, combined with their high affinity toward eIF4E, makes them attractive candidates for stable small molecule inhibitors of translation.

Further studies in the rabbit reticulocyte lysate system have shown that pCCl_2p analogues **2b** and **7b** were potent and stable inhibitors of translation (IC_{50} of 0.97 and 0.95 μM for **2b** and **7b** respectively). The *in vivo* use of nucleoside triphosphates is hampered by their low cell-penetrability associated with the electronegativity of their phosphate units. However, methods for delivery systems/modification strategies have been developed (70–73), which could subsequently be applied for testing the potency of novel cap analogues in cell systems.

The binding and inhibition experiments allowed us to characterize properties of cap analogues as small molecule ligands interacting with eIF4E. However, since the cap is an integral part of an mRNA chain *in vivo*, and *in vitro* transcribed mRNAs gain increasing attention as potential vaccines and gene replacement therapeutics (74), we were also interested in evaluating the novel cap analogues as reagents for modification of 5' end of mRNA, and in the determining the translation efficiencies of mRNAs capped with various modified analogues. Our results are in general agreement with previous observations that high affinity for eIF4E is a necessary but not sufficient condition for efficient translation (40,75), indicating that other factors play a role in defining mRNA translational properties. For instance, the previously described imidodiphosphate modification was found to generally stabilize the eIF4E-cap complex, but produced rather poorly translated mRNAs (75). In fact, the pCCl_2p analogue **7b** described here is the first bridging-oxygen-substitution analogue that does not impair the translational efficiency of mRNA. This signifies the pCCl_2p analogues as potentially useful reagents for the synthesis of *in vitro* transcribed mRNAs with applications in exogenous gene delivery. Moreover, to fully evaluate the usefulness of the halomethylene-containing analogues for mRNA modification, further studies on the susceptibility to hDcp2 pyrophosphatase of transcripts capped with these analogues were performed. It occurred that RNAs capped with cap analogues carrying β/γ -bridging substitution for methylene or halomethylene group are less susceptible to hDcp2 than transcripts capped with tri- or tetraphosphate ARCA. Notably, under the conditions of our assay, RNAs capped with CCl_2 -modified analogue were completely resistant to decapping. Such exceptionally high resistance to decapping by Dcp2 has been previously observed in the case of cap analogs modified with double O-to-S substitutions at the non-bridging positions (2S-analogs) (26). However, the synthesis and purification of 2S analogs is much more challenging, especially because, in contrast to CCl_2 -analogues, they exist in four P-diastereomeric forms. Inter-

estingly, compounds carrying the CCl_2 -modification were also the most resistant to hDcpS activity.

Next, we determined the translational properties of mRNAs capped with dihalomethylene analogues in living cells. The translation efficiencies determined in HeLa cells revealed that mRNA capped with p CCl_2 p analogue **7b** is expressed over 2-fold more efficiently than mRNAs capped with other methylene analogues (**7a** and **7c**), and slightly more efficiently than RNA capped with unmodified tetraphosphate analog, **7d**. However, in contrast to **7d** compound **7b** was resistant to Dcp2, and why this difference appears to little have only influence on mRNA expression is currently unclear to us. Possible explanations require further investigation and may include some HeLa cells-specific effects or interference from other cap-binding proteins or decapping enzymes.

Taken altogether, the dichloromethylene substitution distinguished itself as superior in the context of mRNA properties relevant to therapeutic applications, when compared to all other bridging cap modifications tested so far. This fact, combined with synthetic availability and lack of stereogenic center in the oligophosphate chain modified with p CCl_2 p moiety (in contrast to all non-bridging modifications), makes the analogue **7b** a promising capping reagent for mRNAs produced for *in vivo* applications.

Finally, we have also demonstrated that despite not optimal biochemical properties, the difluoromethylene cap analogues can be applied as molecular tools in cap-related biochemical and biophysical assays. The difluoromethylene analogue **6c** was successfully used as a reporter ligand in ^{19}F NMR based assays, allowing observation of ligand binding to eIF4E as well as the monitoring of DcpS-mediated hydrolysis. We anticipate that in the future these assays might facilitate inhibitor discovery for cap-dependent proteins.

ACCESSION NUMBERS

Structures of eIF4E in complex with m7GppppG (**6d**) (PDB id: 5J5O) and with m27,2'OGpp CCl_2 ppG (**7b**) (PDB id: 5J5Y).

SUPPLEMENTARY DATA

Supplementary Data are available at NAR Online.

ACKNOWLEDGEMENTS

We thank Prof. Mike Kiledjian (Rutgers University) for hDcpS and hDcp2 encoding plasmids and Prof. Stephen R. Ikeda (The National Institute on Alcohol Abuse and Alcoholism) for providing hRLuc-pRNA2(A)128 plasmid.

FUNDING

National Science Center, Poland [UMO-2012/05/E/ST5/03893, UMO-2016/21/B/ST5/02556, UMO-2013/08/A/NZ1/00866]; Ministry of Science and Higher Education, Poland [DI2012 024842]. HPLC and MS measurements were performed in the Biopolymers Laboratory, Division of Biophysics, Institute of Experimental Physics, Faculty of Physics, University of Warsaw, supported by the

ERDF within the Innovation Economy Operational Programme [POIG.02.01.00-14-122/09]. Funding for open access charge: National Science Center, Poland [UMO-2012/05/E/ST5/03893].

Conflict of interest statement. None declared.

REFERENCES

- Shatkin, A.J. (1987) mRNA caps-old and newer hats. *Bioessays*, **7**, 275–277.
- Furuichi, Y. and Shatkin, A.J. (2000) Viral and cellular mRNA capping: past and prospects. *Adv. Virus Res.*, **55**, 135–184.
- Houseley, J. and Tollervy, D. (2009) The Many Pathways of RNA Degradation. *Cell*, **136**, 763–776.
- Ziemiak, M., Strenkowska, M., Kowalska, J. and Jemielity, J. (2013) Potential therapeutic applications of RNA cap analogs. *Future Med. Chem.*, **5**, 1141–1172.
- Jemielity, J., Kowalska, J., Rydzik, A. and Darzynkiewicz, E. (2010) Synthetic mRNA cap analogs with a modified triphosphate bridge—synthesis, applications and prospects. *N. J. Chem.*, **34**, 829–844.
- Karaki, S., Andrieu, C., Ziouziou, H., Rocchi, P. and Donev, R. (2015) The eukaryotic translation initiation factor 4E (eIF4E) as a therapeutic target for cancer. *Adv. Prot. Chem. Struct. Biol.*, **101**, 1–26.
- Siddiqui, N. and Sonenberg, N. (2015) Signalling to eIF4E in cancer. *Biochem. Soc. Trans.*, **43**, 763–772.
- Bhat, M., Robichaud, N., Hulea, L., Sonenberg, N., Pelletier, J. and Topisirovic, I. (2015) Targeting the translation machinery in cancer. *Nat. Rev. Drug Discov.*, **14**, 261–278.
- Graff, J., Konicek, B., Vincent, T., Lynch, R., Monteith, D., Weir, S., Schwier, P., Capen, A., Goode, R., Dowless, M. *et al.* (2007) Therapeutic suppression of translation initiation factor eIF4E expression reduces tumor growth without toxicity. *J. Clin. Invest.*, **117**, 2638–2648.
- Li, S., Jia, Y., Jacobson, B., McCauley, J., Kratzke, R., Bitterman, P. and Wagner, C. (2013) Treatment of breast and lung cancer cells with a N-7 benzyl guanosine monophosphate tryptamine phosphoramidate pronucleotide (4Ei-1) results in chemosensitization to gemcitabine and induced eIF4E proteasomal degradation. *Mol. Pharm.*, **10**, 523–531.
- Hong, D.S., Kurzrock, R., Oh, Y., Wheler, J., Naing, A., Brail, L., Callies, S., Andre, V., Kadam, S.K., Nasir, A. *et al.* (2011) A phase 1 dose escalation, pharmacokinetic, and pharmacodynamic evaluation of eIF-4E antisense oligonucleotide LY2275796 in patients with advanced cancer. *Clin. Cancer Res.*, **17**, 6582–6591.
- Kranz, L., Diken, M., Haas, H., Kreiter, S., Loquai, C., Reuter, K., Meng, M., Fritz, D., Vascotto, F., Hefesha, H. *et al.* (2016) Systemic RNA delivery to dendritic cells exploits antiviral defence for cancer immunotherapy. *Nature*, **534**, 396–401.
- Diken, M., Kreiter, S., Selmi, A., Britten, C., Huber, C., Tureci, O. and Sahin, U. (2011) Selective uptake of naked vaccine RNA by dendritic cells is driven by macropinocytosis and abrogated upon DC maturation. *Gene Ther.*, **18**, 702–708.
- Sahin, U., Kariko, K. and Tureci, O. (2014) mRNA-based therapeutics - developing a new class of drugs. *Nat. Rev. Drug Discov.*, **13**, 759–780.
- Kuhn, A.N., Diken, M., Kreiter, S., Selmi, A., Kowalska, J., Jemielity, J., Darzynkiewicz, E., Huber, C., Tureci, O. and Sahin, U. (2010) Phosphorothioate cap analogs increase stability and translational efficiency of RNA vaccines in immature dendritic cells and induce superior immune responses *in vivo*. *Gene Ther.*, **17**, 961–971.
- van Dijk, E., Cougot, N., Meyer, S., Babajko, S., Wahle, E. and Seraphin, B. (2002) Human Dcp2: a catalytically active mRNA decapping enzyme located in specific cytoplasmic structures. *EMBO J.*, **21**, 6915–6924.
- Wang, Z., Jiao, X., Carr-Schmid, A. and Kiledjian, M. (2002) The hDcp2 protein is a mammalian mRNA decapping enzyme. *Proc. Natl. Acad. Sci. U.S.A.*, **99**, 12663–12668.
- Liu, S.W., Jiao, X., Liu, H., Gu, M., Lima, C.D. and Kiledjian, M. (2004) Functional analysis of mRNA scavenger decapping enzymes. *RNA*, **10**, 1412–1422.
- Taverniti, V. and Seraphin, B. (2015) Elimination of cap structures generated by mRNA decay involves the new scavenger mRNA

- decapping enzyme Aph1/FHIT together with DcpS. *Nucleic Acids Res.*, **43**, 482–492.
20. Grudzien-Nogalska, E. and Kiledjian, M. (2017) New insights into decapping enzymes and selective mRNA decay. *Wiley Interdiscipl. Rev.-RNA*, **8**, doi:10.1002/wrna.1379.
 21. Chang, J.H., Jiao, X., Chiba, K., Oh, C., Martin, C.E., Kiledjian, M. and Tong, L. (2012) Dxo1 is a new type of eukaryotic enzyme with both decapping and 5'-3' exoribonuclease activity. *Nat. Struct. Mol. Biol.*, **19**, 1011–1017.
 22. Jiao, X., Doamekpor, S.K., Bird, J.G., Nickels, B.E., Tong, L., Hart, R.P. and Kiledjian, M. (2017) 5' End nicotinamide adenine dinucleotide cap in human cells promotes RNA decay through DXO-mediated deNADding. *Cell*, **168**, 1015–1027.
 23. Kowalska, J., Lewdorowicz, M., Zuberek, J., Grudzien-Nogalska, E., Bojarska, E., Stepinski, J., Rhoads, R.E., Darzynkiewicz, E., Davis, R.E. and Jemielity, J. (2008) Synthesis and characterization of mRNA cap analogs containing phosphorothioate substitutions that bind tightly to eIF4E and are resistant to the decapping pyrophosphatase DcpS. *RNA*, **14**, 1119–1131.
 24. Kowalska, J., Lukaszewicz, M., Zuberek, J., Darzynkiewicz, E. and Jemielity, J. (2009) Phosphoroselenoate dinucleotides for modification of mRNA 5' end. *ChemBiochem*, **10**, 2469–2473.
 25. Kowalska, J., Wypijewska del Nogal, A., Darzynkiewicz, Z.M., Buck, J., Nicola, C., Kuhn, A.N., Lukaszewicz, M., Zuberek, J., Strenkowska, M., Ziemniak, M. *et al.* (2014) Synthesis, properties, and biological activity of boranophosphate analogs of the mRNA cap: versatile tools for manipulation of therapeutically relevant cap-dependent processes. *Nucleic Acids Res.*, **42**, 10245–10264.
 26. Strenkowska, M., Grzela, R., Majewski, M., Wnek, K., Kowalska, J., Lukaszewicz, M., Zuberek, J., Darzynkiewicz, E., Kuhn, A.N., Sahin, U. *et al.* (2016) Cap analogs modified with 1,2-dithiodiphosphate moiety protect mRNA from decapping and enhance its translational potential. *Nucleic Acids Res.*, **44**, 9578–9590.
 27. Blackburn, G. and Guo, M. (1991) Synthesis, physical, chemical, and enzyme studies on bis-2,6-diaminopurine beta-d-ribofuranoside p1,p4-tetraphosphate. *Nucleosides Nucleotides*, **10**, 549–551.
 28. Blackburn, G. and Langston, S. (1991) Novel p1,p2-substituted phosphonate analogs of 2'-deoxyadenosine and 2'-deoxythymidine 5'-triphosphates. *Tetrahedron Lett.*, **32**, 6425–6428.
 29. Blackburn, G., Guo, M., Langston, S. and Taylor, G. (1990) Novel phosphonate and thiophosphate analogs of ap3a, diadenosine 5',5'''-p1,p3-triphosphate. *Tetrahedron Lett.*, **31**, 5637–5640.
 30. Blackburn, G., Eckstein, F., Kent, D. and Perree, T. (1985) I sopolar vs isosteric phosphonate analogs of nucleotides. *Nucleosides Nucleotides*, **4**, 165–167.
 31. Blackburn, G., Kent, D. and Kolkman, F. (1981) 3 new beta,gamma-methylene analogs of adenosine-triphosphate. *J. Chem. Soc.-Chem. Commun.*, 1188–1190.
 32. Oertell, K., Wu, Y., Zakharova, V., Kashemirov, B., Shock, D., Beard, W., Wilson, S., McKenna, C. and Goodman, M. (2012) Effect of beta,gamma-CHF- and beta,gamma-CHCl-dGTP halogen atom stereochemistry on the transition state of DNA polymerase beta. *Biochemistry*, **51**, 8491–8501.
 33. Upton, T., Kashemirov, B., McKenna, C., Goodman, M., Prakash, G., Kultyshev, R., Batra, V., Shock, D., Pedersen, L., Beard, W. *et al.* (2009) alpha,beta-Difluoromethylene deoxynucleoside 5'-triphosphates: a convenient synthesis of useful probes for DNA polymerase beta structure and function. *Org. Lett.*, **11**, 1883–1886.
 34. Singh, J., Salcius, M., Liu, S.W., Staker, B.L., Mishra, R., Thurmond, J., Michaud, G., Mattoon, D.R., Printen, J., Christensen, J. *et al.* (2008) DcpS as a therapeutic target for spinal muscular atrophy. *ACS Chem. Biol.*, **3**, 711–722.
 35. Wypijewska, A., Bojarska, E., Stepinski, J., Jankowska-Anyska, M., Jemielity, J., Davis, R.E. and Darzynkiewicz, E. (2010) Structural requirements for *Caenorhabditis elegans* DcpS substrates based on fluorescence and HPLC enzyme kinetic studies. *FEBS J.*, **277**, 3003–3013.
 36. Kalek, M., Jemielity, J., Darzynkiewicz, Z.M., Bojarska, E., Stepinski, J., Stolarski, R., Davis, R.E. and Darzynkiewicz, E. (2006) Enzymatically stable 5' mRNA cap analogs: synthesis and binding studies with human DcpS decapping enzyme. *Bioorg. Med. Chem.*, **14**, 3223–3230.
 37. Rydzik, A.M., Lukaszewicz, M., Zuberek, J., Kowalska, J., Darzynkiewicz, Z.M., Darzynkiewicz, E. and Jemielity, J. (2009) Synthetic dinucleotide mRNA cap analogs with tetraphosphate 5',5' bridge containing methylenebis(phosphonate) modification. *Org. Biomol. Chem.*, **7**, 4763–4776.
 38. Kowalska, J., Lukaszewicz, M., Zuberek, J., Ziemniak, M., Darzynkiewicz, E. and Jemielity, J. (2009) Phosphorothioate analogs of m7GTP are enzymatically stable inhibitors of cap-dependent translation. *Bioorg. Med. Chem. Lett.*, **19**, 1921–1925.
 39. Grudzien-Nogalska, E., Stepinski, J., Jemielity, J., Zuberek, J., Stolarski, R., Rhoads, R.E. and Darzynkiewicz, E. (2007) Synthesis of anti-reverse cap analogs (ARCA) and their applications in mRNA translation and stability. *Methods Enzymol.*, **431**, 203–227.
 40. Jemielity, J., Fowler, T., Zuberek, J., Stepinski, J., Lewdorowicz, M., Niedzwiecka, A., Stolarski, R., Darzynkiewicz, E. and Rhoads, R.E. (2003) Novel "anti-reverse" cap analogs with superior translational properties. *RNA*, **9**, 1108–1122.
 41. Cohen, L., Mikhli, C., Friedman, C., Jankowska-Anyska, M., Stepinski, J., Darzynkiewicz, E. and Davis, R. (2004) Nematode M(7)GpppG and m(3)(2,2,7)GpppG decapping: activities in *Ascaris* embryos and characterization of *C-elegans* scavenger DcpS. *RNA*, **10**, 1609–1624.
 42. Zuberek, J., Wyslouch-Cieszyńska, A., Niedzwiecka, A., Dadlez, M., Stepinski, J., Augustyniak, W., Gingras, A., Zhang, Z., Burley, S., Sonenberg, N. *et al.* (2003) Phosphorylation of eIF4E attenuates its interaction with mRNA 5' cap analogs by electrostatic repulsion: Intein-mediated protein ligation strategy to obtain phosphorylated protein. *RNA*, **9**, 52–61.
 43. Niedzwiecka, A., Marcotrigiano, J., Stepinski, J., Jankowska-Anyska, M., Wyslouch-Cieszyńska, A., Dadlez, M., Gingras, A., Mak, P., Darzynkiewicz, E., Sonenberg, N. *et al.* (2002) Biophysical studies of eIF4E cap-binding protein: recognition of mRNA 5' cap structure and synthetic fragments of eIF4G and 4E-BP1 proteins. *J. Mol. Biol.*, **319**, 615–635.
 44. Coleman, T., Wang, G. and Huang, F. (2004) Superior 5' homogeneity of RNA from ATP-initiated transcription under the T7 phi 2.5 promoter. *Nucleic Acids Res.*, **32**, e14.
 45. Williams, D.J., Puhl, H.L. and Ikeda, S.R. (2010) A simple, highly efficient method for heterologous expression in mammalian primary neurons using cationic lipid-mediated mRNA transfection. *Front. Neurosci.*, **4**, 181.
 46. Kabsch, W. (2010) XDS. *Acta Crystallogr. D Biol. Crystallogr.*, **66**, 125–132.
 47. Krug, M., Weiss, M., Heinemann, U. and Mueller, U. (2012) XDSAPP: a graphical user interface for the convenient processing of diffraction data using XDS. *J. Appl. Cryst.*, **45**, 568–572.
 48. McCoy, A., Grosse-Kunstleve, R., Adams, P., Winn, M., Storoni, L. and Read, R. (2007) Phaser crystallographic software. *J. Appl. Cryst.*, **40**, 658–674.
 49. Schüttelkopf, A. and van Aalten, D. (2004) PRODRG: a tool for high-throughput crystallography of protein-ligand complexes. *Acta Cryst. D*, **60**, 1355–1363.
 50. Lebedev, A., Young, P., Isupov, M., Moroz, O., Vagin, A. and Murshudov, G. (2012) J.Ligand: a graphical tool for the CCP4 template-restraint library. *Acta Cryst. D*, **68**, 431–440.
 51. Emsley, P. and Cowtan, K. (2004) Coot: model-building tools for molecular graphics. *Acta Cryst. D*, **60**, 2126–2132.
 52. Adams, P., Afonine, P., Bunkoczi, G., Chen, V., Davis, I., Echols, N., Headd, J., Hung, L., Kapral, G., Grosse-Kunstleve, R. *et al.* (2010) PHENIX: a comprehensive Python-based system for macromolecular structure solution. *Acta Cryst. D*, **66**, 213–221.
 53. Nikolovska-Coleska, Z., Wang, R., Fang, X., Pan, H., Tomita, Y., Li, P., Roller, P., Krajewski, K., Saito, N., Stuckey, J. *et al.* (2004) Development and optimization of a binding assay for the XIAP BIR3 domain using fluorescence polarization. *Anal. Biochem.*, **332**, 261–273.
 54. Leung, I., Demetriades, M., Hardy, A., Lejeune, C., Smart, T., Szollosi, A., Kawamura, A., Schofield, C. and Claridge, T. (2013) Reporter ligand NMR screening method for 2-oxoglutarate oxygenase inhibitors. *J. Med. Chem.*, **56**, 547–555.
 55. Stepinski, J., Waddell, C., Stolarski, R., Darzynkiewicz, E. and Rhoads, R.E. (2001) Synthesis and properties of mRNAs containing the novel "anti-reverse" cap analogs 7-methyl(3'-O-methyl)GpppG and 7-methyl(3'-deoxy)GpppG. *RNA*, **7**, 1486–1495.
 56. Zuberek, J., Jemielity, J., Jablonowska, A., Stepinski, J., Dadlez, M., Stolarski, R. and Darzynkiewicz, E. (2004) Influence of electric charge

- variation at residues 209 and 159 on the interaction of eIF4E with the mRNA 5' terminus. *Biochemistry*, **43**, 5370–5379.
57. Liu, H., Rodgers, N.D., Jiao, X. and Kiledjian, M. (2002) The scavenger mRNA decapping enzyme DcpS is a member of the HIT family of pyrophosphatases. *EMBO J.*, **21**, 4699–4708.
 58. Gu, M., Fabrega, C., Liu, S.W., Liu, H., Kiledjian, M. and Lima, C.D. (2004) Insights into the structure, mechanism, and regulation of scavenger mRNA decapping activity. *Mol. Cell*, **14**, 67–80.
 59. Wypijewska, A., Bojarska, E., Lukaszewicz, M., Stepinski, J., Jemielity, J., Davis, R.E. and Darzynkiewicz, E. (2012) 7-methylguanosine diphosphate (m(7)GDP) is not hydrolyzed but strongly bound by decapping scavenger (DcpS) enzymes and potentially inhibits their activity. *Biochemistry*, **51**, 8003–8013.
 60. She, M., Decker, C.J., Chen, N., Tumati, S., Parker, R. and Song, H. (2006) Crystal structure and functional analysis of Dcp2p from *Schizosaccharomyces pombe*. *Nat. Struct. Mol. Biol.*, **13**, 63–70.
 61. Kalek, M., Jemielity, J., Grudzien, E., Zuberek, J., Bojarska, E., Cohen, L.S., Stepinski, J., Stolarski, R., Davis, R.E., Rhoads, R.E. *et al.* (2005) Synthesis and biochemical properties of novel mRNA 5' cap analogs resistant to enzymatic hydrolysis. *Nucleos. Nucleot. Nucleic Acids*, **24**, 615–621.
 62. Kitevski-LeBlanc, J. and Prosser, R. (2012) Current applications of F-19 NMR to studies of protein structure and dynamics. *Progr. Nucl. Magn. Reson. Spectr.*, **62**, 1–33.
 63. Dalvit, C., Fagerness, P., Hadden, D., Sarver, R. and Stockman, B. (2003) Fluorine-NMR experiments for high-throughput screening: theoretical aspects, practical considerations, and range of applicability. *J. Am. Chem. Soc.*, **125**, 7696–7703.
 64. Chen, H., Viel, S., Ziarelli, F. and Peng, L. (2013) F-19 NMR: a valuable tool for studying biological events. *Chem. Soc. Rev.*, **42**, 7971–7982.
 65. Lindon, J.C. and Wilson, I.D. (2015) *eMagRes*. John Wiley & Sons, Ltd, Vol. **4**.
 66. Smith, A., Zhang, Z., Pielak, G. and Li, C. (2015) NMR studies of protein folding and binding in cells and cell-like environments. *Curr. Opin. Struct. Biol.*, **30**, 7–16.
 67. Veronesi, M., Giacomina, F., Romeo, E., Castellani, B., Ottonello, G., Lambruschini, C., Garau, G., Scarpelli, R., Bandiera, T., Piomelli, D. *et al.* (2016) Fluorine nuclear magnetic resonance-based assay in living mammalian cells. *Anal. Biochem.*, **495**, 52–59.
 68. Baranowski, M.R., Nowicka, A., Rydzik, A.M., Warminski, M., Kasprzyk, R., Wojtczak, B.A., Wojcik, J., Claridge, T.D., Kowalska, J. and Jemielity, J. (2015) Synthesis of fluorophosphate nucleotide analogues and their characterization as tools for ¹⁹F NMR studies. *J. Org. Chem.*, **80**, 3982–3997.
 69. Howell, M., Singh, N. and Singh, R. (2014) Advances in therapeutic development for spinal muscular atrophy. *Future Med. Chem.*, **6**, 1081–1099.
 70. Moore, M.J. (2005) From birth to death: the complex lives of eukaryotic mRNAs. *Science*, **309**, 1514–1518.
 71. Zochowska, M., Piguet, A., Jemielity, J., Kowalska, J., Szolajska, E., Dufour, J. and Chroboczek, J. (2015) Virus-like particle-mediated intracellular delivery of mRNA cap analog with in vivo activity against hepatocellular carcinoma. *Nanomed.-Nanotechnol. Biol. Med.*, **11**, 67–76.
 72. Gollnest, T., de Oliveira, T., Schols, D., Balzarini, J. and Meier, C. (2015) Lipophilic prodrugs of nucleoside triphosphates as biochemical probes and potential antivirals. *Nat. Commun.*, **6**, 8716.
 73. Wagner, C., Iyer, V. and McIntee, E. (2000) Pronucleotides: toward the in vivo delivery of antiviral and anticancer nucleotides. *Med. Res. Rev.*, **20**, 417–451.
 74. Vallazza, B., Petri, S., Poleganov, M., Eberle, F., Kuhn, A. and Sahin, U. (2015) Recombinant messenger RNA technology and its application in cancer immunotherapy, transcript replacement therapies, pluripotent stem cell induction, and beyond. *Wiley Interdiscipl. Rev.-RNA*, **6**, 471–499.
 75. Rydzik, A.M., Kulis, M., Lukaszewicz, M., Kowalska, J., Zuberek, J., Darzynkiewicz, Z.M., Darzynkiewicz, E. and Jemielity, J. (2012) Synthesis and properties of mRNA cap analogs containing imidodiphosphate moiety-fairly mimicking natural cap structure, yet resistant to enzymatic hydrolysis. *Bioorg. Med. Chem.*, **20**, 1699–1710.